Journal of Thermal Analysis and Calorimetry, Vol. 90 (2007) 3, 849–857

CRYSTALLIZATION BEHAVIOR OF ISOTACTIC POLYPROPYLENE BASED NANOCOMPOSITES

V. Causin[1*], *Carla Marega*[1], *Roberta Saini*[1], *A. Marigo*[1] *and G. Ferrara*[2]

[1]Dipartimento di Scienze Chimiche, Universitŕ di Padova, via Marzolo 1, 35131 Padova, Italy
[2]Basell Poliolefine Italia SpA – Centro Ricerche 'Giulio Natta', P.le Donegani 12, 44100 Ferrara, Italy

The effect of clay dispersion on the crystallization behavior of isotactic polypropylene (iPP)-based nanocomposites is reported. The T_m^0 of the materials was calculated by the method proposed by Marand, the kinetics of crystallization was evaluated by the Avrami analysis and also the Hoffman-Lauritzen theory of crystallization regimes was applied. Montmorillonite was found to depress T_m^0, to enhance the rate of crystallization and to ease the chain folding of macromolecules. These effects were magnified if clay was exfoliated, rather than intercalated.

Keywords: *DSC, montmorillonite, nanocomposites, polypropylene, SAXS, thermal analysis, WAXD*

Introduction

The large potential in property improvement associated to the addition of small fractions of nanofiller in a polymer matrix has aroused a relevant amount of research in the academic and industrial community. Montmorillonite (MMT) is a very commonly employed nanofiller. It is a smectite-type clay with a layered structure; each layer is 1 nm thick and has side dimensions ranging from 30 nm to several microns or more [1, 2]. The performance of polymer-clay nanocomposites strongly depends on the breaking-up of clay particles in the polymer matrix. As the degree of interaction between polymer and filler varies, three systems are generally found: clay sheets may remain stacked in structures called tactoids, as in the original mineral without any improvement compared to usual microcomposites with a low filler loading; polymer chains may penetrate into interlayer spacing, producing an intercalated system where clay layers are more separated; finally, an exfoliated structure could appear, with the single clay sheets delaminated and dispersed in the matrix. The latter system is the most desirable since nanometric dispersion of clay platelets ensures a maximization of the interfacial region between the filler and the polymer matrix, and a consequent improvement in reinforcement effect.

In the last 50 years, isotactic polypropylene (iPP) has become one of the most widespread commodities, employed in the industry due to its low cost and good mechanical performance [3]. The development of nanocomposites based on this polymer would thus be of critical importance for the industrial diffusion of such a novel class of materials. A particular characteristic of iPP is its polymorphic behaviour, as it is known that this polymer has three different crystalline phases: α, β and γ [4]. Polymorphism is important for technological reasons, because each phase has different physical and mechanical characteristics. The monoclinic α phase is the best known and the most common crystalline state of the polymer. On the other hand, the hexagonal β phase and the orthorhombic γ phase can be obtained only in particular conditions [5, 6].

The aim of obtaining exfoliation has been successfully accomplished with polar polymers such as polyamides, but the considerable difference in polarity between polyolefins like iPP and clay posed serious problems in preparing satisfactory nanocomposites based on this latter class of polymers. To improve the interaction between the components of the system, clay is usually modified by cationic surfactants to make it more organophilic, while compatibilizers such as maleated PP (mPP) or processing aid agents are added to iPP to reduce its apolarity or improve its mobility [7–9].

Physical mechanical properties are not the only aspect of this class of polymer-based materials that undergo changes. The structure of the polymer and its thermal behavior also vary significantly as a consequence of the addition of the filler and of the compatibilizing and processing aid agents [10–19]. The effect of montmorillonite on the crystallization kinetics of iPP is somewhat controversial. Most researchers [12, 13] observed an increase in crystallization rate brought about by clay, while other groups found that the filler slowed it down [20] or had no ef-

* Author for correspondence: valerio.causin@unipd.it

1388–6150/$20.00
© 2007 Akadémiai Kiadó, Budapest
Akadémiai Kiadó, Budapest, Hungary
Springer, Dordrecht, The Netherlands

fect [14] on the kinetics. Not many works appeared in the literature where the effect of filler dispersion was accounted for [15, 18].

Another effect that has not so far been well studied is that of the filler on the equilibrium melting temperature (T_m^0). This quantity corresponds to the melting temperature of a large stack of perfect extended chain crystals. T_m^0 is very important because, for an accurate study of crystallization kinetics, the supercooling ΔT, i.e. the difference between T_m^0 and the crystallization temperature T_c, must be known. The difference in free energy between melt and crystal phases depends in fact on ΔT, so only comparing polymers crystallized at the same ΔT one can be sure that they experienced the same driving force for crystallization. Very few estimates of T_m^0 of iPP-based nanocomposites are available in the literature. Maiti *et al.* [14] investigated mPP nanocomposites with montmorillonite and found that either the matrix and the composites shared the same T_m^0 of 158°C. An increase in T_m^0 of nanocomposites with respect to neat iPP was on the other hand reported by Ma *et al.* [12].

In this work T_m^0 was estimated according to the method proposed and applied by Marand *et al.* [21–23], which has been shown to correct some of the flaws that affect the commonly used Hoffman-Weeks procedure [24]. Subsequently the kinetics of the samples was studied according to the Avrami theory [25–27] and compared as a function of undercooling. The surface free energy of folding was also evaluated by the Hoffman-Lauritzen equation [28, 29], thus obtaining an estimate of the ease with which polymer chains can fold in the samples considered.

Transmission Electron Microscopy (TEM), Polarized Light Optical Microscopy (PLOM), Wide Angle X-Ray Diffraction (WAXD) and Small Angle X-Ray Scattering (SAXS) have been used to characterize the structure and morphology of the samples, whereas their thermal behavior was studied by DSC.

Experimental

Materials

Samples and sample preparation

Two commercially available grades of homopolymer produced by Basell Polyolefins S.p.A. were used, as described elsewhere [8]. The first is Moplen HP 500J, hereafter denoted as sample J, with a melt flow rate of 3.2 g/10 min (corresponding to $\underline{M}_w$ =390000) and a flexural modulus of 1500 MPa. The second one is Moplen HP 500N, hereafter denoted as sample N), with a melt flow rate of 12 g/10 min (corresponding to $\underline{M}_w$ =250000) and a flexural modulus around 1550 MPa.

Nanocomposites contained 5% of Cloisite 15-A, montmorillonite ion-exchanged with octadecylammonium ions, produced by Southern Clay Products. Two different agents were added to the polymer: the first one (denoted ka) was Hifax KA805, a polymer based on mPP containing approximately 0.7 mass% of grafted maleic anhydride used as compatibilizing agent, the second one (denoted ab) was a processing aid agent, Abriflo 65 (Abril Industrial Waxes Ltd.), based on monoethanolstereamide. In each case the amount of added agent was 7 mass%.

The components were mixed in a reciprocating single screw extruder, Buss MDK 70. The pellets obtained were subsequently processed by injection moulding in accordance with ISO 294-1 or ISO 294-3. The first letter in the designation of the samples, J or N, indicates the polymer base employed, the second identifies the additive (ab=Abriflo or ka=mPP).

Methods

Differential scanning calorimetry

All the measurements were carried out with a TA Instruments mod. 2920 calorimeter operating under N_2 atmosphere. Polymer samples weighing about 5 mg closed in aluminum pans were used throughout the experiments. Indium and tin of high purity were used for calibrating the DSC temperature and enthalpy scales.

Structural and morphological characterization

Reflection WAXD patterns were recorded by a Philips X'Pert PRO diffractometer equipped with a graphite monochromator on the diffracted beam (CuK_α radiation), in the 1.5–40° 2θ angular range. SAXS spectra of the samples were recorded by a Mbraun system, utilizing the CuK_α radiation from a Philips PW 1830 X-ray generator. The data were collected by a position sensitive detector, in the scattering angular range 0.1–5.0° 2θ and they were successively corrected for blank scattering. Finally, the Lorentz correction was applied: $I_1(s)=4\pi s^2 I(s)$, where $I_1(s)$ is the one-dimensional scattering function and $I(s)$ the desmeared intensity function, being $s=(2/\lambda)\sin\theta$. TEM analyses were performed by a TECNAI 10 FEI. Samples were stained by RuO_4 and cryomicrotomed into sections about 100 nm thick. PLOM observations were made with a Leica DM4000M microscope, between crossed polarizers. Tiny pieces of the samples were put on microscope slides, covered with a cover slip, melted at 200°C for 10 min and subsequently crystallized in a Mettler FP82HT Hotstage preset at the desired T_c. Micrographs were taken by a Leica DFC280 digital camera.

Equilibrium melting temperature

The T_m^0 of the samples was determined by the technique proposed by Marand *et al.* [21–23]. After erasure of thermal history at 200°C for 5 min, samples were rapidly brought to the desired T_c and allowed to crystallize for a time t_c, and subsequently heated to 200°C at 10°C min^{-1} (Fig. 1). The instrumental drift associated to the rapid jump towards crystallization temperature (T_c) was estimated by running a DSC experiment with an inert Al_2O_3 sample of the same mass (5 mg) as that used for polymer samples. Crystallization temperatures were chosen so that the induction time before the beginning of crystallization was larger than the time requested by the apparatus to recover from the instrumental drift.

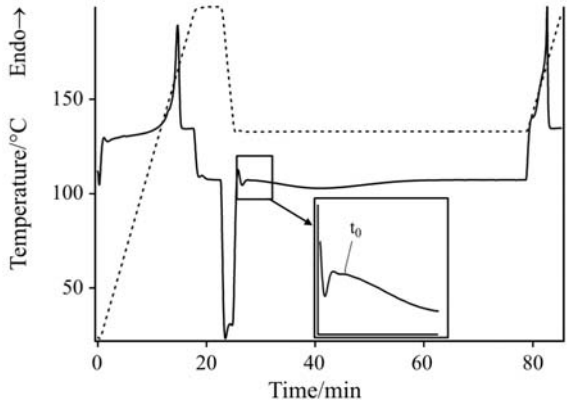

Fig. 1 DSC trace (solid line) and temperature (dashed line, left axis) as a function of time in a typical isothermal crystallization experiment (sample Nab, T_c=134°C). In the inset, the choice of the induction time t_0 is shown

The peak maximum of the melting endotherm was taken as the melting point. Although the maximum temperature is somewhat less accurate than the onset point, being influenced by sample size, the use of specimens of approximately the same mass allowed for the employment of the former parameter. Peak temperature was used by the researchers that previously measured the T_m^0 of iPP-based nanocomposite samples [12, 14], on samples approximately the same size as those used in this work [12], so its choice was dictated also by the need of obtaining data comparable with the literature. For each T_c, crystallization was repeated for six or seven different t_c's, using the same sample to avoid the effect of sample preparation. A prior evaluation of resistance to thermal degradation was made according to Juhász *et al.* [23]. By TG experiments, performed on a TA Instruments SDT 2960 apparatus, it was moreover checked that the onset of degradation was located beyond 200°C. On the basis of these data it was possible to obtain the melting temperature of initial and non-thickened lamellae, T_m, by extrapolation to the induction time t_0. t_0 has been evaluated as the time when the first deviation of the thermogram baseline is detected (Fig. 1). Variables $X=T_m^0/(T_m^0-T_c)$ and $M=T_m^0/(T_m^0-T_m)$ were thus evaluated with tentative T_m^0 values and each time a M *vs.* X plotted to verify the following expression [21]:

$$M=\gamma(X+a) \quad (1)$$

γ is the thickening coefficient, that tends to 1 in the absence of thickening phenomena, i.e. at the beginning of crystallization. a is a dimensionless term that accounts to the non-linearity of T_m–T_c data.

Kinetics of crystallization

The kinetics of crystallization was studied by subjecting each sample to the following thermal cycle: after erasure of previous thermal history by keeping the polymer at 200°C for 5 min, it was cooled at the maximum rate to the crystallization temperature (T_c). The heat evolved during the transition was monitored as a function of time during an isothermal at T_c of suitable length. The fraction X of material crystallized after the time t was estimated from the relation:

$$X=\int_0^t\left(\frac{dH}{dt}\right)dt\Big/\int_0^\infty\left(\frac{dH}{dt}\right)dt \quad (2)$$

where the numerator is the heat generated at time t and the denominator is the total heat of crystallization. The Avrami equation [25–27] was used to correlate X with time:

$$X=1-\exp[-K(t-t_0)^n] \quad (3)$$

K is the kinetic constant of crystallization, n is a coefficient linked to the time dependence and the dimensions of growth of crystallites.

Hoffman-Lauritzen analysis

The crystallization behavior of the polymer was also studied according to the relationship between chain folded crystal growth rate and undercooling proposed by Hoffman and Lauritzen [28, 29]:

$$\ln G+\frac{U^*}{R(T_c-T_\infty)}=\ln G_0-\frac{K_g}{T_c\Delta Tf} \quad (4)$$

where G is the crystal growth rate, U^* is a constant characteristic of the activation energy for repetitive chain motion and is equal to 1500 cal mol^{-1}, R is the gas constant, $T_\infty=T_g-30$, T_g being the glass transition temperature, f is a correction factor equal to $2T_c/(T_m+T_c)$ and G_0 is a pre-exponential factor.

The constant K_g is given by:

$$K_g = \frac{jb_0\sigma\sigma_e}{k\Delta H} \quad (5)$$

where j is an integer equal to 2 in the second regime of crystallization and to 4 in the first and third regime of crystallization, b_0 is the thickness of the surface layer, σ and σ_e are the interfacial free energies of the lateral and fold surface, respectively, k is the Boltzmann constant and ΔH is the enthalpy of fusion per mole of repeat units.

Results and discussion

The degree of dispersion of the filler in the polymer matrix was evaluated by WAXD, SAXS and TEM [8]. As the degree of interaction between polymer and clay varies, montmorillonite can attain three different structures. When polymer chains do not interact with the filler, clay layers remain stacked in structures called tactoids and retain the spacing they had in pristine montmorillonite. These tactoids will be called immiscible in the rest of the paper and are characterized by XRD signals, either in WAXD and SAXS experiments, located at the same angular position as pristine montmorillonite. When polymer chains may penetrate into interlayer spacing, intercalated tactoids are formed, that give rise to WAXD and SAXS signals shifted towards small angles, with respect to the original filler. Finally, exfoliation can not be detected by WAXD or SAXS, because the ordered stacking of the layers is disrupted. Figure 2 shows the WAXD diffractograms of the four considered nanocomposites compared to that of pristine montmorillonite.

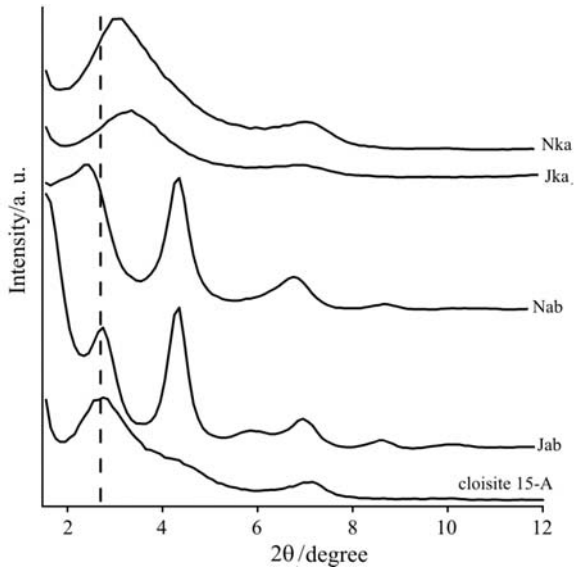

Fig. 2 WAXD patterns of the considered composites and of the pristine cloisite filler. The dashed vertical line corresponds to the periodicity of pure cloisite

As may be seen, when mPP was used as a compatibilizing agent a small increase in the angular position of the basal signal of clay was detected. This corresponds to clay layers collapsing, probably as a consequence of processing that brought about the degradation of the cationic surfactant used in the organomodified clay. In the case of samples prepared with the processing aid agent, on the other hand, WAXD data showed that some of the clay tactoids retained the same spacing as in pristine montmorillonite. Samples were also studied by SAXS (Fig. 3). In mPP-compatibilized samples, Jka and Jab, just one peak, correspondent to the interlayer distance of pristine cloisite, was observed. Two peaks appeared for sample Jab, one assignable to immiscible tactoids, i.e. with the same periodicity as pristine cloisite, and one originated by intercalated tactoids, with an interlayer distance of 59 Ĺ. In the case of Nab a single, very broad signal was observed, ascribable to a quite wide distribution of interlayer distances between 30 Ĺ and about 60 Ĺ, i.e. a wide range of tactoids exist in this sample, some of them 'immiscible', the others intercalated at different degrees. Figure 4 shows TEM micrographs of samples obtained with mPP and the processing aid agent. As may be seen, only in the case of mPP compatibilized composites exfoliated layers are visible, whereas when Abriflo was used clay is dispersed in the matrix in tactoids. Nanocomposites produced with mPP have thus a morphology characterized by the coexistence of 'immiscible' tactoids, in which interaction with the polymer determined only a reduction in the number of stacked layers but not an enlargement of interlayer distance, and exfoliated single layers. On the other hand, the use of Abriflo as a processing aid agent could not enable the achievement of exfoliation, so in samples Nab and Jab the filler appeared stacked in 'immiscible' and intercalated tactoids. It should be noted that both immiscible and intercalated tactoids have a small number of layers, about 10, as previously reported [30] and as can be seen in TEM pictures, dramatically less than the

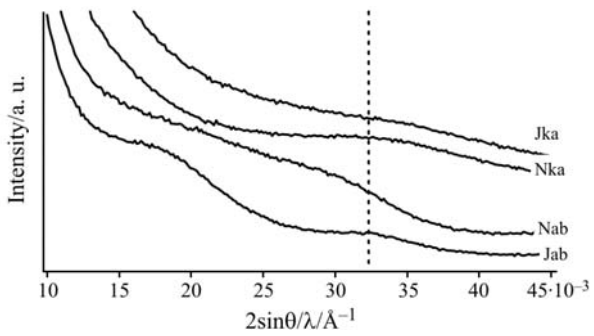

Fig. 3 SAXS patterns of the considered composites. The dashed vertical line corresponds to the periodicity of pure cloisite

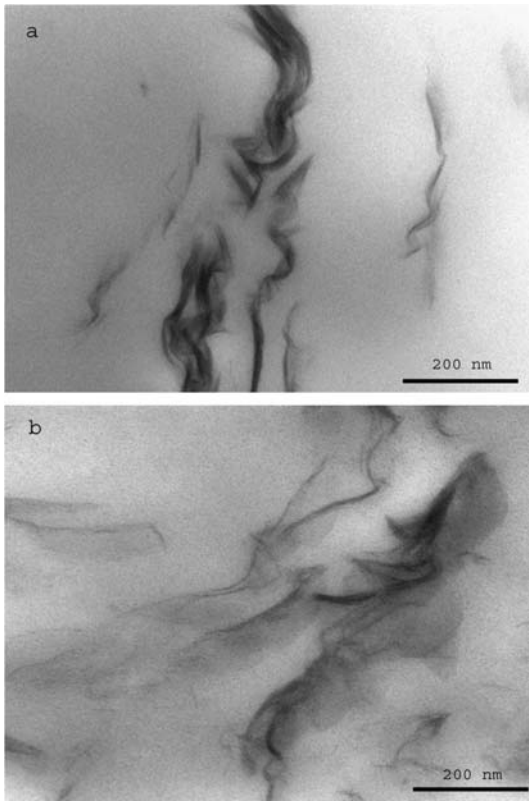

Fig. 4 TEM micrographs of samples a – Jab and b – Nka

hundreds or thousands that compose pristine stacks. Knowledge of the morphology of the studied composites was important for the study of a correlation between structure and thermal properties in these materials.

The commonly employed procedure for estimating T_m^0 is based on the Hoffman and Weeks approach [24]. Marand *et al.* [21, 22] however recently showed that this procedure tends to underestimate the actual T_m^0 of polymers. This effect is particularly evident in iPP, for which a wide range of T_m^0's has been proposed, varying from 186 to 212°C [31–35].

It is known that the extent of lamellar thickening depends both on T_c and on crystallization time [21, 33, 36, 37]. In order to rule out the disturbing effect of lamellar thickening, the melting point of initial, non thickened lamellae (T_m) was estimated. The measurement of this initial T_m was obtained by extrapolation at the induction time, defined as the time when the first deviation of the thermogram baseline is detected (Fig. 1). As described in the 'Experimental' section, crystallization at each T_c was performed for different times t_c, so that a peak melting temperature *vs*. logt_c diagram could be plotted and, by linear regression, the extrapolation to t_0 could be calculated [23]. Table 1 shows for each sample t_0 and T_m corresponding to each T_c. Comparing the composites to the base polymers it can be seen that t_0 decreases significantly, a sign that a nucleating effect can be associated to the addition of montmorillonite [14].

On the basis of the data in Table 1, variables M and X were computed as described in the 'Experimental' section and for each tentative T_m^0 graphs such as that in Fig. 5 were drawn. Each of these datasets was fitted by Eq. (1) and the so obtained γ parameter was plotted as a function of T_m^0 (Fig. 6). Since the melting point of non-thickened lamellae was employed in the calculation, the true value of T_m^0 is that for which γ equals to one. Table 2 summarizes the obtained results. The T_m^0 for the matrix polymers J and N are in good agreement with the values reported in the literature [22, 34, 35]. All the composites had a remarkably lower T_m^0 than their corresponding base polymer. This is consistent with a disrupting role of MMT. It has been in fact widely reported that tactoids and clay layers hinder the ordering of macromolecular chains, that thus form less perfect crystals [12–14]. A depression of the melting point as a consequence of the addition

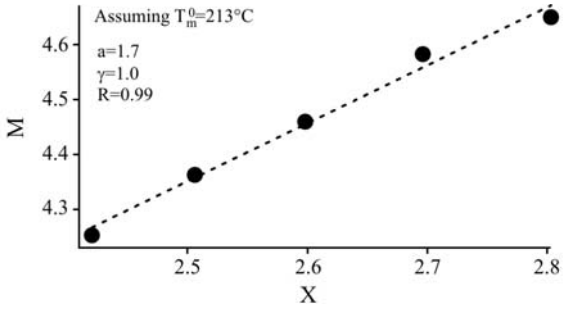

Fig. 5 Plot of *M vs. X* for sample J, assuming=213°C

Table 1 Crystallization temperatures (T_c), induction times (t_0) and melting points of original lamellae (T_m) of all the examined samples

J			Jab		Jka		N		Nab		Nka	
T_c/°C	t_0/min	T_m/°C	t_0/min	T_m/°C	t_0/min	T_m/°C	t_0/min	T_m/°C	t_0/min	T_m/°C	t_0/min	T_m/°C
125	0.39	162.9	0.13	162.8	0.07	163.4	0.5	163.8	0.24	164.5	0.05	163.8
128	0.63	164.2	0.46	163.8	0.14	163.9	0.7	164.4	0.4	164.4	0.1	163.6
131	1.43	165.2	0.69	164.1	0.31	164.3	1.51	165.3	0.7	165.2	0.3	164.3
134	1.74	166.5	1.44	165.4	1.19	164.7	1.62	165.5	1.2	164.2	0.8	166.3
137	2.97	167.2	2.64	166.7	1.47	166.5	2.3	167.0	2	167.0	1	167.0

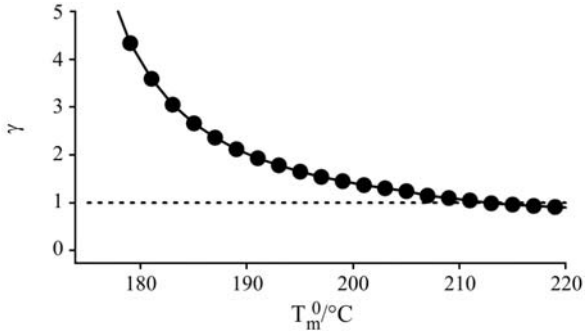

Fig. 6 Dependence of γ on the choice of T_m^0 for sample J

Table 2 Equilibrium melting temperatures of the considered samples

Sample	T_m^0/°C
J	213
Jab	208
Jka	197
N	214
Nab	205
Nka	195

of MMT was found by Svoboda and coworkers [15] and by Kim *et al.* [18]. Arroyo *et al*. found that T_m^0 of iPP decreased when short glass fibers were added [38]. Varma-Nair and Agarwal measured the T_m^0 of iPP samples treated with nucleants and reported a decrease in the equilibrium melting temperature in nucleated polymers [39]. The decrease of T_m^0 in nanocomposites seems correlated to the degree of filler dispersion. The largest depression of T_m^0 was observed in samples compatibilized with mPP, in which exfoliation occurred. In the case of exfoliation, the interfacial area is greatly increased with respect to the intercalated system. The extent of the polymer-filler interface influences the crystallization behavior of the matrix polymers and it is therefore not surprising that the extent of the effects of the filler is magnified when exfoliation occurs. It must be said that also the compatibilizer or the processing aid agent could have an effect on T_m^0. It seems reasonable though to attribute the main role to clay, as Seo *et al.* [10] reported that mPP brings about an increase in T_m^0. Since the observed equilibrium melting temperature of the composites was significantly lower than that of the base polymers, it must be concluded that, if present, the effect of the compatibilizer was overwhelmed by that of the nanofiller.

The kinetics of crystallization was studied by DSC. Figure 7 shows the development of relative crystallinity for one of the samples, when crystallized at different T_c's. As T_c decreases, crystallization proceeds at a faster rate. The quantification of the kinetics was carried out according to the Avrami theory, obtaining plots like those of Fig. 8. The fitting was performed on the central linear portions of the datasets, as at longer times large deviations due to the onset of secondary crystallization are very visible. In some occasions also some points in the short time regions were not considered because logarithmic plotting tended to overestimate small errors in the assessment of the initial time of crystallization [10]. Table 3 shows the results of the Avrami analysis. An *n* of about 2 was found for samples J, N and Nka, indicative of 2-dimensional growth with simultaneous nucleation [40, 41]. The base polymers exhibited *n* values in accord with literature data on neat iPP [42]. Non-integer values of *n* were obtained for the other samples. This may be explained by phenomena like the partial overlapping of primary nucleation on crystal growth [43, 44], mixed crystallization modes [45], diffusion controlled growth [38, 45] or a non constant growth [10]. The *n*'s of samples Jab, Jka and Nka lied in an interval between 2 and 3, indicative of heterogeneous nucleation associated to diffusion controlled growth [44]. A trend was observed in composites towards increasing *n* that may be associated to a change from instantaneous to sporadic nucleation [10 and references therein]. Nucleants are known to bring about an increase in *n* values [10, 12, 19, 38, 46].

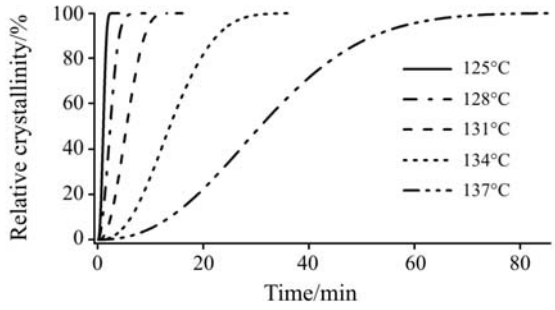

Fig. 7 Development of relative crystallinity with time for isothermal crystallization of sample Nab at 125, 128, 131, 134 and 137°C

Figure 9 shows the trend of the kinetic constant *K* as a function of Δ*T*. Once again, three groups can be

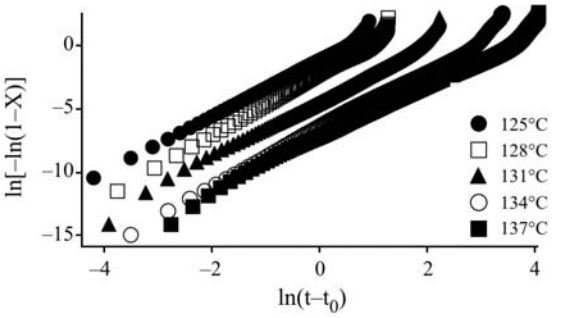

Fig. 8 Avrami plots of sample Nka isothermally crystallized at different temperatures

Table 3 Avrami parameters for J-based and N-based samples

J			Jab			Jka		
ΔT	n	ln$K$	ΔT	n	ln$K$	ΔT	n	ln$K$
88	2.24	–1.45	83	2.26	–1.35	72	2.54	–1.17
85	2.02	–3.91	80	2.51	–3.01	69	2.03	–2.57
82	1.90	–5.22	77	2.44	–5.46	66	2.64	–4.02
79	2.00	–6.75	74	2.53	–7.76	63	2.74	–6.89
76	2.02	–8.40	71	2.73	–10.73	60	2.69	–8.99

N			Nab			Nka		
ΔT/°C	n	ln$K$	ΔT/°C	n	ln$K$	ΔT/°C	n	ln$K$
89	1.93	–1.6	80	2.55	–1.03	70	2.20	–1.16
86	2.19	–2.56	77	2.35	–1.92	67	2.01	–2.01
83	1.89	–3.89	74	2.23	–4.05	64	2.16	–4.10
80	1.62	–4.73	71	2.29	–6.26	61	2.25	–6.75
77	1.79	–6.18	68	2.23	–7.97	58	1.93	–7.08

singled out: the base polymers, intercalated and exfoliated composites. The fastest rate was observed for nanocomposites compatibilized with mPP, the slowest in samples J and N. The nucleating activity of MMT was therefore greatest if the filler was exfoliated, while it appeared somewhat reduced when it was intercalated. PLOM micrographs confirm this observation. Figures 10–12 show that the spherulite dimension and order decrease passing from the base polymer, to the intercalated Abriflo-containing sample, to the exfoliated, mPP-compatibilized nanocomposite. No significant change in the morphology of spherulites was observed, even though the appearance of fibrillar structures has been previously reported [13]. This was expected, since the limited changes observed in the Avrami n exponents did not allow to infer radical changes in the dimensionality of crystal growth.

The issue of whether MMT actually accelerates iPP crystallization is still controversial. A number of studies confirmed that this filler acts as a nucleant [12, 13], but others reported a retarded kinetics [20] or also no effect [14]. The role of the compatibilizer in determining this effect is likely to be minor, because acceleration of the rate has been observed either in compatibilized and non-compatibilized systems [20]. Svoboda and coworkers [15] observed a nucleation be-

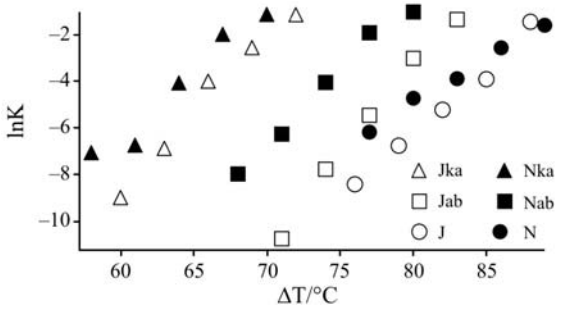

Fig. 9 Variation of the Avrami kinetic constant of crystallization K as a function of undercooling

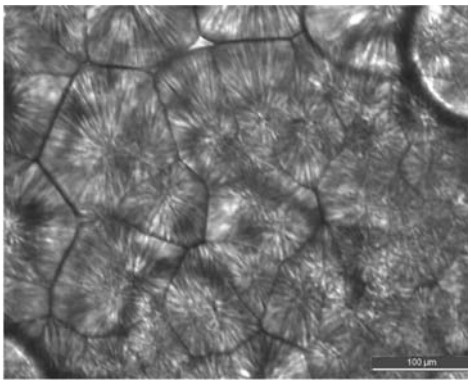

Fig. 10 PLOM micrograph of sample J crystallized at 134°C

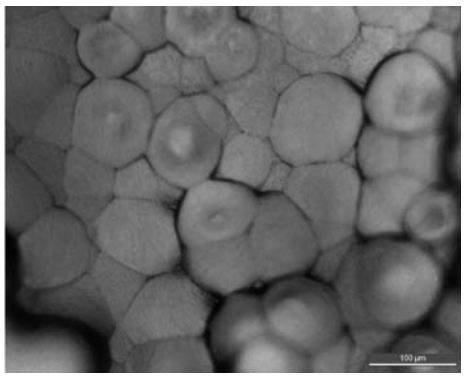

Fig. 11 PLOM micrograph of sample Nab crystallized at 134°C

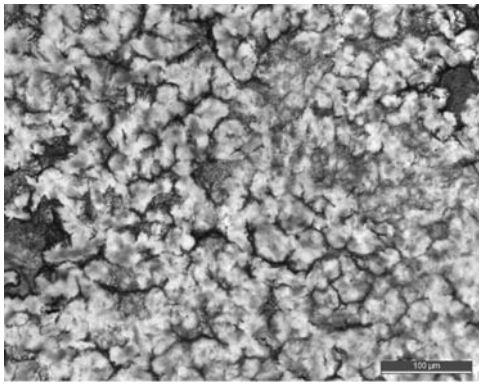

Fig. 12 PLOM micrograph of sample Jka crystallized at 134°C

havior associated to the presence of tactoids, that was lost in the case of well dispersed, exfoliated clay layers. Similar results were found by Kim *et al.* [18] who observed an increase in the crystallization rate for agglomerated or intercalated systems, while exfoliated nanocomposites crystallized more slowly than the base polymer. This was ascribed to a diffusion barrier enacted by clay layers, but also to the release of the organic modifier that may hinder crystallization. The reason for this dissimilar results may be that in our case comparisons were made on the basis of undercooling, while most reported data are compared as a function of T_c. For instance, if sample Nka and N crystallized at 137°C are compared, the base polymer has a ln$K$ of –6.18, while the exfoliated composite has a lower kinetic constant ln$K$= –7.08. It must also be remarked that in the samples studied in this work exfoliated or intercalated layers coexist with a small fraction of immiscible tactoids. As can be seen in Fig. 3b, though, there are just a few tactoids, and exfoliated layers should be considered the key components defining the interfacial area, and the crystallization behavior, in mPP composites. One of the reasons for this increase in the rate of crystallization could be found in the mechanism itself of crystallization. The interfacial free energy σ_e, that may be estimated by the Hoffman-Lauritzen theory, is directly proportional to the work of chain folding, and can then be used as a measure for evaluating how easy it is for macromolecules to fold into lamellae. Figure 13 shows the Hoffman-Lauritzen plots obtained for the considered samples. No significant break in the slope was observed, signifying that no change in crystallization regime occurs in the considered temperature range. As the undercoolings employed in this work are considerably larger than the threshold value for the II→III regime transition (48°C) [31], it was assumed that the polymers in this study crystallized according to regime III. So substituting 4, $6.26\cdot10^{-8}$ cm, 11.5 and $1.96\cdot10^{9}$ erg cm^{-3} respectively for j, b_0, σ and ΔH in Eq. (5) [47], σ_e values (Table 4) could be calculated from K_g obtained by fitting the lines of Fig. 13. Concerning the base polymers, it

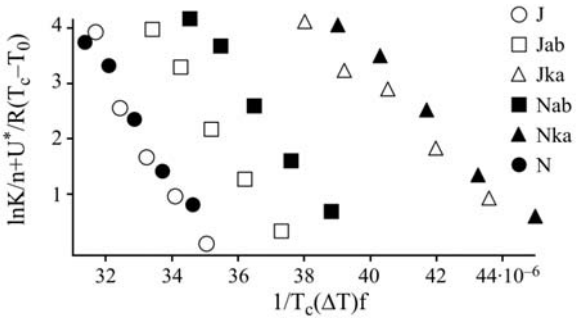

Fig. 13 Hoffman-Lauritzen plots for the considered samples

Table 4 Interfacial free energies of the fold surface for the samples considered

Sample	$\sigma_e/10^5$·J cm^{-2}
J	2.11
Jab	1.86
Jka	1.12
N	1.84
Nab	1.66
Nka	1.22

can be seen that J has a larger σ_e than N. Even more interesting is to compare σ_e values of the composites relative to the matrix. σ_e decreases significantly for intercalated nanocomposites and even more for exfoliated ones. This means that chain folding is favored in exfoliated composites more than in intercalated ones and the base polymers. This effect on the work of chain folding may be one of the reasons for the increase in crystallization rate as the interfacial area is widened. Similar results have previously been reported for traditional composites [39, 46] and nanocomposites [12, 48].

Conclusions

The effect of dispersion of clay layers on the crystallization behavior of iPP-based nanocomposites with montmorillonite was investigated, since it is known that addition of nanosized fillers to a polymer matrix brings about significant changes in its structure and thermal behavior [7, 10–19, 49–51]. Three series of samples were available: base polymers, intercalated and exfoliated nanocomposites. Exfoliated and intercalated systems were found to depress the T_m^0 of the materials, due to the disrupting effect of MMT on the orderly crystallization of the polymer. If on one hand clay does not allow the attainment of a more ordinate structure and morphology with respect to the neat matrix, on the other hand MMT favors the kinetics of crystallization. This can be attributed to the lowering of the work of chain folding associated to the formation of nanocomposites. When the clay was exfoli-

ated, the effect was much enhanced with respect to that of intercalated systems, so it is reasonable to think that the role of the filler on the crystallization behavior is linked to the extent of the interfacial region between polymer and filler.

Acknowledgments

V. C. is grateful to the University of Padova for financial support.

References

1 S. S. Ray and M. Okamoto, Prog. Polym. Sci., 28 (2003) 1539.
2 W. Shao, Q. Wang and H. Ma, Polym. Int., 54 (2005) 336.
3 E. P. Moore, Polypropylene Handbook, Hanser, Cincinnati 1996.
4 A. Turner Jones, J. M. Aizlewood and D. R. Beckett, Makromol. Chem., 75 (1964) 134.
5 A. Marigo, C. Marega, V. Causin and P. Ferrari, J. Appl. Polym. Sci., 91 (2004) 1008.
6 A. Marigo, V. Causin, C. Marega and P. Ferrari, Polym. Int., 53 (2004) 2001.
7 M. Alexander and P. Dubois, Mater. Sci. Eng., 28 (2000) 1.
8 E. M. Benetti, V. Causin, C. Marega, A. Marigo, G. Ferrara, A. Ferraro, M. Consalvi and F. Fantinel, Polymer, 46 (2005) 8275.
9 L. A. Utracki, M. Sepehr and J. Li, Int. Polym. Proc., 21 (2006) 3.
10 Y. Seo, J. Kim, K. U. Kim and Y. C. Kim, Polymer, 41 (2000) 2639.
11 A. Pozsgay, T. Fráter, L. Papp, I. Sajó and B. Pukánszky, J. Macromol. Sci. Phys., B41 (2002) 1249.
12 J. Ma, S. Zhang, Z. Qi, G. Li and Y. Hu, J. Appl. Polym. Sci., 83 (2002) 1978.
13 S. Hambir, N. Bulakh and J.P. Jog, Polym. Eng. Sci., 42 (2002) 1800.
14 P. Maiti, P. H. Nam, M. Okamoto, N. Hasegawa and A. Usuki, Macromol., 35 (2002) 2042.
15 P. Svoboda, C. Zeng, H. Wang, L. J. Lee and D. L. Tomasko, J. Appl. Polym. Sci., 85 (2002) 1562.
16 R. Nowacki, B. Monase, E. Piorkowska, A. Galeski and J. M. Haudin, Polymer, 45 (2004) 4877.
17 L. Wang, J. Sheng and S. Wu, J. Macromol. Sci. Phys., 43 (2004) 935.
18 B. Kim., S.-H. Lee, D. Lee, B. Ha, J. Park and K. Char, Ind. Eng. Chem. Res., 43 (2004) 6082.
19 G. Xu, W. Shi, P. Hu and S. Mo, Eur. Polym. J., 41 (2005) 1828.
20 A. Somwangthanaroj, E. C. Lee and M. J. Solomon, Macromol., 36 (2003) 1333.
21 H. Marand, J. Xu and S. Srinivas, Macromol., 31 (1998) 8219.
22 J. Xu, S. Srinivas, H. Marand and P. Agarwal, Macromol., 31 (1998) 8230.
23 P. Juhász, J. Varga, K. Belina and H. Marand, J. Therm. Anal. Cal., 69 (2002) 561.
24 J. D. Hoffman and J. J. Weeks, J. Res. Natl. Bur. Stand. U.S.A., A66 (1962) 13.
25 M. Avrami, J. Chem. Phys., 7 (1939) 1103.
26 M. Avrami, J. Chem. Phys., 8 (1940) 212.
27 M. Avrami, J. Chem. Phys., 9 (1941) 177.
28 J. I. Jr. Lauritzen and J. D. Hoffman, Treatise on Solid State Chemistry, Ed.: N. B. Hannay, Plenum Press, New York 1976, Vol. 3.
29 J. I. Jr. Lauritzen and J. D. Hoffman, J. Appl. Phys., 44 (1973) 4340.
30 V. Causin, C. Marega, A. Marigo and G. Ferrara, Polymer, 46 (2005) 9533.
31 S. Z. D. Cheng, J. J. Janimak, A. Zhang and H. N. Cheng, Macromol., 23 (1990) 298.
32 W. F. Krigbaum and I. Uematsu, J. Polym. Sci. Polym. Phys. Ed., 3 (1965) 767.
33 K. Mezghani, R. A. Campbell and P. J. Phillips, Macromol., 27 (1994) 997.
34 J. G. Fatou, Eur. Polym. J., 7 (1971) 1057.
35 B. Monnasse and J. M. Handin, Colloid Polym. Sci., 263 (1985) 822.
36 K. Kamide and K. Yamaguchi, Makromol. Chem., 162 (1972) 205.
37 K. Kamide and K. Yamaguchi, Makromol. Chem., 162 (1972) 219.
38 M. Arroyo, M.A. Lopez-Manchado and F. Avalos, Polymer, 38 (1997) 5587.
39 M. Varma-Nair and P. K. Agarwal, J. Therm. Anal. Cal., 59 (2000) 483.
40 J. Yin, S. Wang and Y. Zhang, J. Polym. Sci. Polym. Phys. Ed., 43 (2005) 1914.
41 C. A. Avila-Orta, C. Burger, R. Somani, L. Yang, G. Marom, F. J. Medellin-Rodriguez and B. S. Hsiao, Polymer, 46 (2005) 8859.
42 C. A. Hieber, Polymer, 36 (1995) 1455.
43 L. Mandelkern, Crystallization of Polymers, McGraw-Hill, New York 1964.
44 L. Valentini, J. Biagiotti, J. M. Kenny and M. A. López Manchado, J. Appl. Polym. Sci., 89 (2003) 2657.
45 B. Wunderlich, Macromolecular Physics, Academic Press, New York 1976.
46 M. Mucha and Z. Królikowski, J. Therm. Anal. Cal., 74 (2003) 549.
47 A. A. Alwattari and D. R. Lloyd, Polymer, 39 (1998) 1129.
48 W. Xu, M. Ge and P. He, J. Polym. Sci. Polym. Phys. Ed., 40 (2002) 408.
49 M. Avella, S. Cosco, M. L. Di Lorenzo, E. Di Pace and M. E. Errico, J. Therm. Anal. Cal., 80 (2005) 131.
50 D.-Y. Yang, Q.-X. Liu, X.-L. Xie and F.-D. Zeng, J. Therm. Anal. Cal., 84 (2006) 355.
51 C. J. Pérez, V. A. Alvarez, P. M. Stefani and A. Vásquez, J. Therm. Anal. Cal., DOI:10.1007/s10973-005-7466-1

Received: September 26, 2006
Accepted: October 19, 2006
OnlineFirst: February 26, 2007

DOI: 10.1007/s10973-006-8205-y